Numerical Simulation of Dispersal of Inert Seeding Material in Israel Using a Three-Dimensional Mesoscale Model

ZEV LEVIN, SHIMON O. KRICHAK, AND TAMIR REISIN

Department of Geophysics and Planetary Science, Tel Aviv University, Ramat Aviv, Israel

(Manuscript received 18 January 1996, in final form 25 September 1996)

ABSTRACT

A mesoscale model RAMS (the Regional Atmospheric Modeling System) was used to investigate the effectiveness of the broadcast static seeding method for dispersing particles into clouds, as it is used in Israel. The model was run using three nested grids, with 500 m × 500 m horizontal resolution in the finest grid. In this paper, the particles were assumed to be inert; namely, only the wind field controlled the dispersal of the tracer particles, and no interaction with cloud or precipitation particles was considered. Although the resolution of the model is good for mesoscale studies, it could not resolve individual plumes. The results, therefore, present average values of the concentrations at each level. The simulations showed that seeding particles reach altitudes at which they could become effective as ice nuclei. These cases were primarily the ones in which the updrafts developed over the seeding lines when the seeding plane was just passing underneath. In these cases only, seeding at about 1-km level (~4°C) with 500 g h^{-1} of inert material (simulating AgI particles) resulted in about 1×10^3–2×10^3 L^{-1} being lifted to the −10°C level. Based on previous laboratory studies of the seeding agent used in Israel, out of these total concentrations, only 1–2 L^{-1} could form ice at −10°C. The simulations also suggest that in most other cases the horizontal advection diluted the particles in the air and only very low concentrations ($<10^{-3}$ L^{-1}, active at −10°C) reached the −10°C level. Most other released particles were transported horizontally with the winds and were later on forced down by downdrafts. Although these simulations await some experimental verification, they suggest that the broadcast seeding method used in Israel is not so effective for widespread rain enhancement operations.

1. Introduction

The Israeli Rain Enhancement project has been in operation for more than 30 years. In spite of the fact that some measure of success has been reported (Gagin and Neumann 1974, 1981; Gabriel and Rosenfeld 1990), there are still questions about the effectiveness of the seeding method used and about its applicability to the Israeli project or to other projects elsewhere. In addition, a recent report by Gabriel and Rosenfeld (1990) suggested that seeding in the southern region of the experiment resulted in no measurable effect. A number of hypotheses have been suggested to explain the lack of seeding effect in the southern region. Overseeding by natural ice nuclei (IN) during dust storms has been suggested as one possible reason for the lack of rain enhancement by artificial seeding (Rosenfeld and Farbstein 1992). Others (Levin et al. 1990; Levin 1994) have suggested that the presence of giant hygroscopic nuclei in the form of dust coated with sulfate could explain the lack of positive seeding effects in the south. This last suggestion is based on the observation that the large drops formed by giant cloud condensation nuclei (CCN) accelerate the collision-coalescence process and reduce the importance of the ice particles in rain formation. In addition, upon ascent to subfreezing levels, ice multiplication could occur by the Hallett and Mossop (1974) mechanism. It is also possible that the formation of high supersaturations with respect to water and ice, due to the reduction in surface area caused by the decrease in the concentrations of the small drops, could increase ice nucleation (Hussain and Saunders 1984).

One point that has only been partially addressed relates to the effectiveness of the dispersal method of the seeding material in the Israeli project. In the Israeli Rain Enhancement project, the broadcast ''static'' seeding method has been employed. Using this method, seeding material is dispersed from airplanes along fixed lines located upwind of the target areas, with the expectation that the winds will carry the AgI particles to the regions in the clouds in which they could be activated as IN.

The issue of the appropriate locations of the seeding lines with respect to the target areas was more recently addressed by Gagin and Aroyo (1985). They calculated the distance from the target area to the seeding line by the use of a simple Gaussian plume dispersal method. The criterion for choosing the seeding line was that the

Corresponding author address: Prof. Zev Levin, J. Goldemberg Chair in Atmospheric Physics, Dept. of Geophysics and Planetary Science, Tel Aviv University, Ramat Aviv 69978 Israel.
E-mail: zev@hail.tau.ac.il

TABLE 1. Model setup.

	First grid	Second grid	Third grid
Horizontal dimensions (No. of points: long., lat.)	36 × 28	58 × 100	128 × 74 north 158 × 74 south
Horizontal grid size (km)	21	3	0.5 × 0.5
Vertical dimension (number of points)	24 km (18)	24 km (18)	24 km (18)
Vertical grid size (m)	300 m minimum, stretching up to 1000 m	300 m minimum, stretching up to 1000 m	300 m minimum, stretching up to 1000 m
Time step (s)	90	22.5	2.2
Top boundary conditon	Rigid wall	Rigid wall	Rigid wall
Lateral boundary	Davies (1983)	Clark and Farley (1984)	Clark and Farley (1984)
Clouds treatment	Convective, large-scale parameterization	Full microphysics	Full microphysics
Radiation	Short- and longwave (Mahrer and Pielke 1977)	Short- and longwave (Mahrer and Pielke 1977)	Short- and longwave (Mahrer and Pielke 1977)

dispersal should be conducted at such a distance that particles active at -10°C could reach the corresponding altitudes over the target area in concentrations greater than about 10–30 L^{-1}. It was assumed that while the particles moved with the horizontal winds, they would also be carried by updrafts into the clouds and reach the altitudes and temperatures at which they could be effective as ice nuclei. Their calculations, however, did not include a number of important factors that are known to affect the airflow and the dispersal of the seeded material. For example, no consideration was given to the effects of topography on the trajectories of the particles, to the fact that clouds and rain are present during the time of seeding, to the effects of the vertical wind shear, or to the diurnal and seasonal variations in the wind field pattern.

Furthermore, Tzivion et al. (1989) recently demonstrated that effective dispersal of seeding material strongly depends on the seeding altitude and the stage (time) of the development of the cloud. Therefore, seeding in the broadcast static mode, as it is done in Israel, could result in the loss of a large fraction of the particles, even before they enter the clouds, due to dry deposition by downdrafts and wet deposition through scavenging by raindrops. Seeding along the preset lines with winds blowing in the wrong direction could also lead to advection of the seeding material to other areas, possibly contaminating the control or the buffer regions.

It is therefore important to 1) estimate the fraction of seeding material that would manage to reach the proper levels in the clouds and 2) evaluate the activation of these particles as ice nuclei at these heights and assess their effect on rain development. In this paper, we only address the first point by simulating a number of typical meteorological cases using the Regional Atmospheric Modeling System (RAMS) mesoscale model. In the present study, the airflow and cloud development over Israel are simulated. The airborne seeding is simulated in a manner similar to the method used in Israel, namely, dispersal along predetermined lines and at times based on the Israeli seeding criteria. Since only the first question above was to be addressed, the simulation was carried out using inert, noninteracting particles as tracers.

2. The model

The three-dimensional mesoscale model of the Colorado State University–RAMS (see Pielke et al. 1992 for a review) was used to test the effectiveness of the dispersal of seeding material using the Israeli static seeding procedure. The model is fully elastic, employing the quasi-Boussinesq approximation described by Dutton and Fichtl (1969) for deep convection, and is integrated using the ''time-split'' numerical technique. A ''sigma-*z*''-type terrain following coordinate system is employed. The nine predictive variables include the three Cartesian velocity components, the Exner function, ice–liquid water potential temperature, and mixing ratios of total water, rainwater, snow, ice crystals, and graupel particles. Details of the model parameters employed are given in Table 1.

The model was used with a three-domain interactive nested grid system. The ''coarse mesh'' grid of 36 × 28 points with a 21-km increment covered a large part of the eastern Mediterranean region. The second, ''middle'' grid consisted of 58 × 100 points with a 3-km horizontal grid size (see Fig. 1a). It covered most of the area of Israel and some adjacent regions. The third fine mesh grid had a resolution of 500 m × 500 m. In the northern area, a mesh of 128 × 74 points was used (Fig. 1b), while for the experiment in the southern area, we used 158 × 74 points (Fig. 1c). The three grids had 24 levels along the sigma-*z* vertical coordinate in the atmosphere with a spacing of 300 m near the surface, stretching to 1000 m near the model top (about 18 km). Because the modeled area in the south was larger, computer memory restrictions forced us to reduce the number of vertical levels to 16. Five more levels were allocated for the description of the soil processes. The physical processes considered and the methods used for their parameterization were taken from the standard package of the RAMS model and are listed in Table 1.

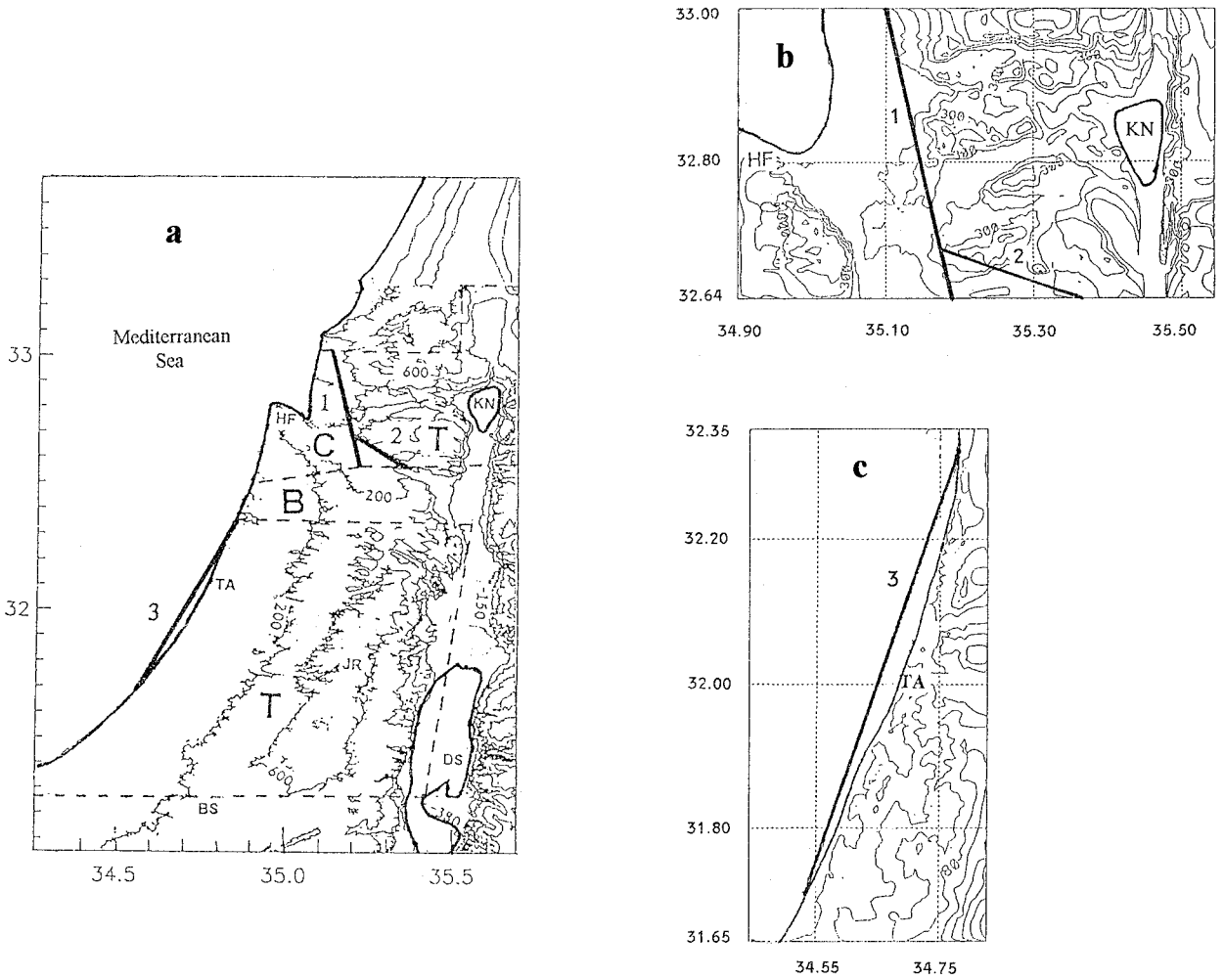

FIG. 1. A map of the seeded regions in Israel (as in the Israel II experiment) including the topography as used in the simulations. (a) The map using the middle grid. (b) and (c) The maps using the inner grids for the regions in the north and the south, respectively. The numbered solid lines represent the three seeding lines adapted in the simulations. The areas bounded by dashed lines represent the north and south targets (T), the buffer zone (B), and the control area (C). The towns of Haifa, Tel Aviv, Jerusalem, and Beer Sheva, Israel, as well as Lake Kineret and the Dead Sea, are marked as HF, TA, JR, BS, KN, and DS, respectively.

The microphysical parameterization scheme in the model was activated in order to describe the development processes of rain, ice, snow, and graupel particles. The initial and time-dependent lateral boundary data for the model consisted of the objective analysis data on a $2.5° \times 2.5°$ grid from the European Centre for Medium-Range Weather Forecasts (ECMWF) at 1000, 850, 700, 500, 300, 200, and 100 hPa. A high-resolution topography of 500 m $\times$ 500 m for Israel (Hall 1993) was imbedded in a coarser topography of 10-min resolution (from the U.S. Navy) used for the outer regions of the model domain. A bilinear interpolation technique was adapted for accurately merging the two topographical datasets. Simulations were conducted on two postfrontal rainy days in Israel.

The specific conditions of the eastern Mediterranean region are characterized by the fact that rain-producing systems develop over the area mainly during the cool season (mid-September–mid-May). During this period, the upper-tropospheric westerly jet stream defines the large-scale structure of the wind field in the region to the south of the area of interest. Westerlies exist in the region of the jet in the troposphere above 700 hPa. Westerly winds in the lower troposphere are normally much stronger during the winter period than during the autumn and spring.

3. Method of simulation

The simulation experiments for each case consisted of two stages. The first stage was to run the model without any simulation of the seeding. Results of the computations during this stage were used in order to determine the proper time for seeding, in accordance with the Israeli seeding criteria, which will be discussed below. The second stage involved a repetition of the

model run with the inclusion of the dispersal process. The simulation of the release of the seeding material was performed in the fine grid only. The simulation of the dispersion was carried out at an altitude similar to the one used in Israel (~1000 m). The three seeding lines (shown in Fig. 1a) were also chosen to mimic the routes of the flights being used in the Israeli project. The coordinates of the starting and final points of each of the seeding lines are as follows:

1) Two lines in the northern region—from 32.65°N, 32.18°E to 32.55°N, 35.40°E and from 33.01°N, 35.17°E to 32.58°N, 35.20°E;
2) one line in the southern region—from 32.20°N, 34.50°E to 31.41°N, 34.33°E.

In Fig. 1, we also included the topography from the digitized data and, identified by dashed lines, the target areas (T) in the north and south, as well as the control (C) and buffer (B) regions in the Israel II experiment.

The criteria for seeding in the Israeli project require the existence, over the target area or entering it, of a convective cloud system deep enough to reach at least the −8°C level. The appropriate seeding lines are then chosen based on the wind direction at the 700-hPa level and the seeding levels (cloud base), as measured by the radiosonde at Beit Dagan, Israel, in the central part of the country (released daily at 0000 and 1200 UTC). Winds from the west to northwest dictate that seeding must be carried out along line 1 in the north and line 3 in the south. When the right clouds exist but the winds are from the southwest, seeding is performed along line 2 in the north, but usually not in the south for fear that the particles would contaminate the buffer region. On occasions with winds from the west-southwest, both seeding lines 1 and 2 are used.

Seeding was simulated in the following way. The airplane was depicted as a point source moving with a speed of 60 m s^{-1} back and forth along the seeding line, dispersing 500 g of AgI every hour. Analysis of the Israeli seeding generators by the Colorado State University (CSU)[1] shows that with a release rate of 7.8 g min^{-1} about 1.4×10^{15} ice crystals per gram are produced at −20°C. The number decreases exponentially with an increase in temperature so that at −15°C the number is 10^{13} g^{-1}, at −10°C it decreases to 10^{12} g^{-1}, and at −8°C it is only 10^{11} g^{-1}. With an inner horizontal grid size of 500 m × 500 m, a vertical grid size at the dispersing level of 450 m, and $\Delta t = 2.2$ s, about 4×10^3 L^{-1} were dispersed every time step. It is important to note that based on the laboratory report quoted above, out of all the particles released, only a small fraction (10^{-3}) or about 4 L^{-1} are active at the −10°C level.

[1] An unpublished report from 1974 provided to EMS, Inc. (in charge of the Israeli seeding operations), graciously given to us by EMS and P. Demott of CSU.

4. Results

Although real meteorological data were used for the initiation of the simulations, it was not the intent of this work to accurately mimic specific cases. The main objective was to obtain a qualitative agreement with cloud fields during the cool and rainy period of the year in the eastern Mediterranean (winter). Two cases were chosen for our simulations. They represent cyclonic activity over Israel that fulfills the seeding criterion. The results of the simulations discussed below show a qualitative agreement with real patterns of cloud fields and motion over Israel. We have no way of knowing if the result of the simulations give the correct cloud parameters, such as vertical winds, liquid water content, etc.

a. Case 1: 1 February 1985

The synoptic conditions in the eastern Mediterranean at the start of the simulation of case 1 are shown in Fig. 2 (surface map at 0000 UTC). A cyclonic system that developed over the central and northern regions of the eastern Mediterranean penetrated the area, having westerly winds in the lower troposphere over Israel. The core of the upper-tropospheric jet, as it appears on a 35°E meridional cross section of objective analysis data, was located over 26°N (with a maximum of 58 m s^{-1}) at the time of the start of the simulation. Wind velocity in the jet over Israel was much lower (about 20 m s^{-1}). Westerly flow existed throughout the troposphere over the area of the simulation. Sea surface temperature was 15°C. In this simulation, convective clouds developed rapidly over the northern part of Israel. Seeding was simulated along lines 1 and 2 for a duration of 6 h, starting 30 min after the beginning of the simulation.

Figure 3a presents a horizontal cross section at 2961 m of the total condensate (g kg^{-1}) associated with cloud development over the northern region (in the inner grid), 1 h after the beginning of the run (30 min after the start of the seeding). These were very deep clouds that moved from the sea to the land, mostly over the northern region including the target area. The results indicate that cloud base was at about 900 m MSL, but that some clouds, especially those farther inland, had bases as high as 1500 m MSL. Some cloud tops reached levels of about 6500 m MSL (temperature approximately −28°C). Total condensate in the clouds reached about 3 g kg^{-1} in the levels between 5000 and 6000 m.

Seeding material spread eastward and slightly northward from lines 1 and 2. The cross section at a height of about 1300 m MSL (Fig. 3b) shows that concentrations of approximately 10^3–10^4 L^{-1} covered small parts of the target area. Concentrations as high as 1.2×10^4 L^{-1} are found near the points at which the planes are present. These high concentrations correspond to the total particles found at these levels. The concentration of the particles that are active at −10°C, for example, is three orders of magnitude lower.

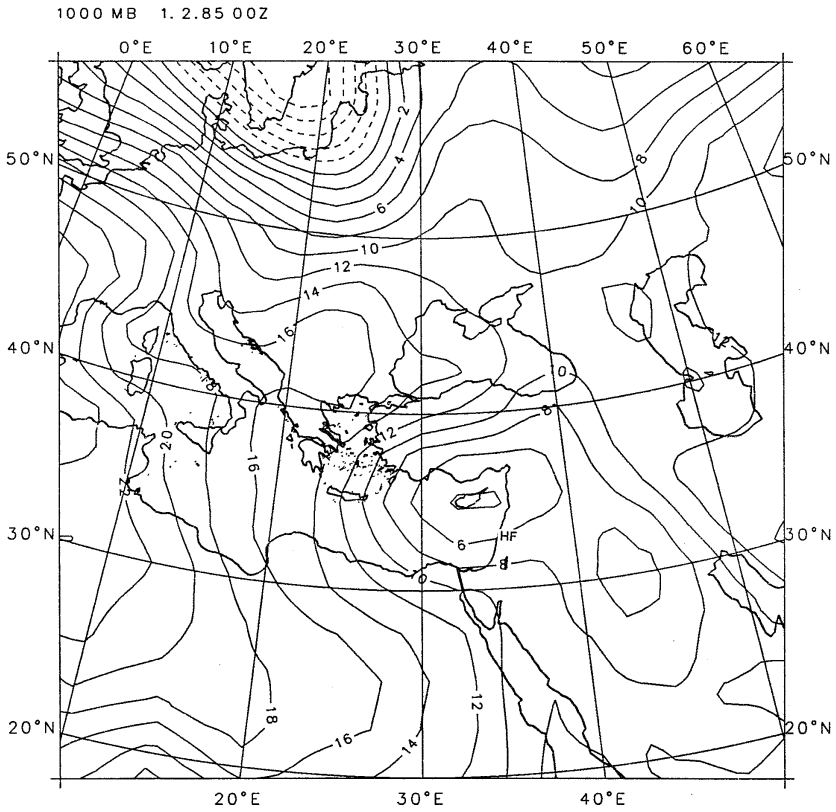

FIG. 2. Synoptic map at 0000 UTC 1 February 1985 at 1000-hPa isobaric height. Isolines are presented every 2 hPa.

The orientation of the plume from line 1 is a result of the horizontal displacement of the seeded particles by the winds after their release. At a later time, when the plane flying along line 1 turned around and headed northward, a new plume was formed from the southernmost point. These particles were again displaced by the winds and formed a plume oriented from southeast to northwest.

Even though the winds advected the particles eastward, vertical transport was somewhat limited. A horizontal cross section at 2961 m (~ -8°C), (Fig. 3c) shows that seeding material reached these levels in a very small region. The maximum total concentration of particles that reached this level was about 10^3 L^{-1}. Of these, only 1 L^{-1} could form ice at -10°C. The penetration into this cloud had occurred about 15 min earlier, when the updraft was located very close to the seeding plane. Other clouds that were formed upwind of the seeding line but crossed it when the plane was not sufficiently close did not carry seeded particles to their upper reaches. The results suggest that most particles were dispersed horizontally and were later deposited or found at lower levels, probably due to downdrafts. Figure 3d shows a vertical cross section of the distribution of the seeded particles along an east–west cross section (see dashed line in Fig. 3c) near the region of maximum concentrations. This vertical section indicates that some seeding material had been entrained into an updraft and remained within the cloud. Concentrations were 2×10^3 L^{-1} at 1500 m MSL ($\sim +2$°C) and 10^3 L^{-1} (i.e., about 1 L^{-1} active at -10°C) up to as high as 4500 m MSL. However, over the rest of the region, most seeding material remained in the lower levels. Figure 3e (466 m MSL) indicates high concentrations of tracer well below cloud base. In the absence of scavenging by rain, it is clear that the high concentrations close to the surface are the result of downdrafts. At 0130, about 1 h after the start of seeding, the clouds moved farther east, and relatively few particles remained underneath them to be lifted. In other words, the continuous release of particles by the seeding plane upwind of the clouds did not increase the particle concentrations near the clouds located far downwind from the seeding lines.

b. Case 2: 26 February 1985

Figure 4 presents the surface map (0000 UTC) for the second case studied. A cyclonic system was present in the eastern Mediterranean along the North African coast. Northwesterly winds in the lower troposphere existed at the time of the start of the simulation. The core of the upper-tropospheric jet was located over 28°N on the 35°E cross section (with a maximum of 70 m s^{-1}). In this case, the sea surface temperature was about 15°C.

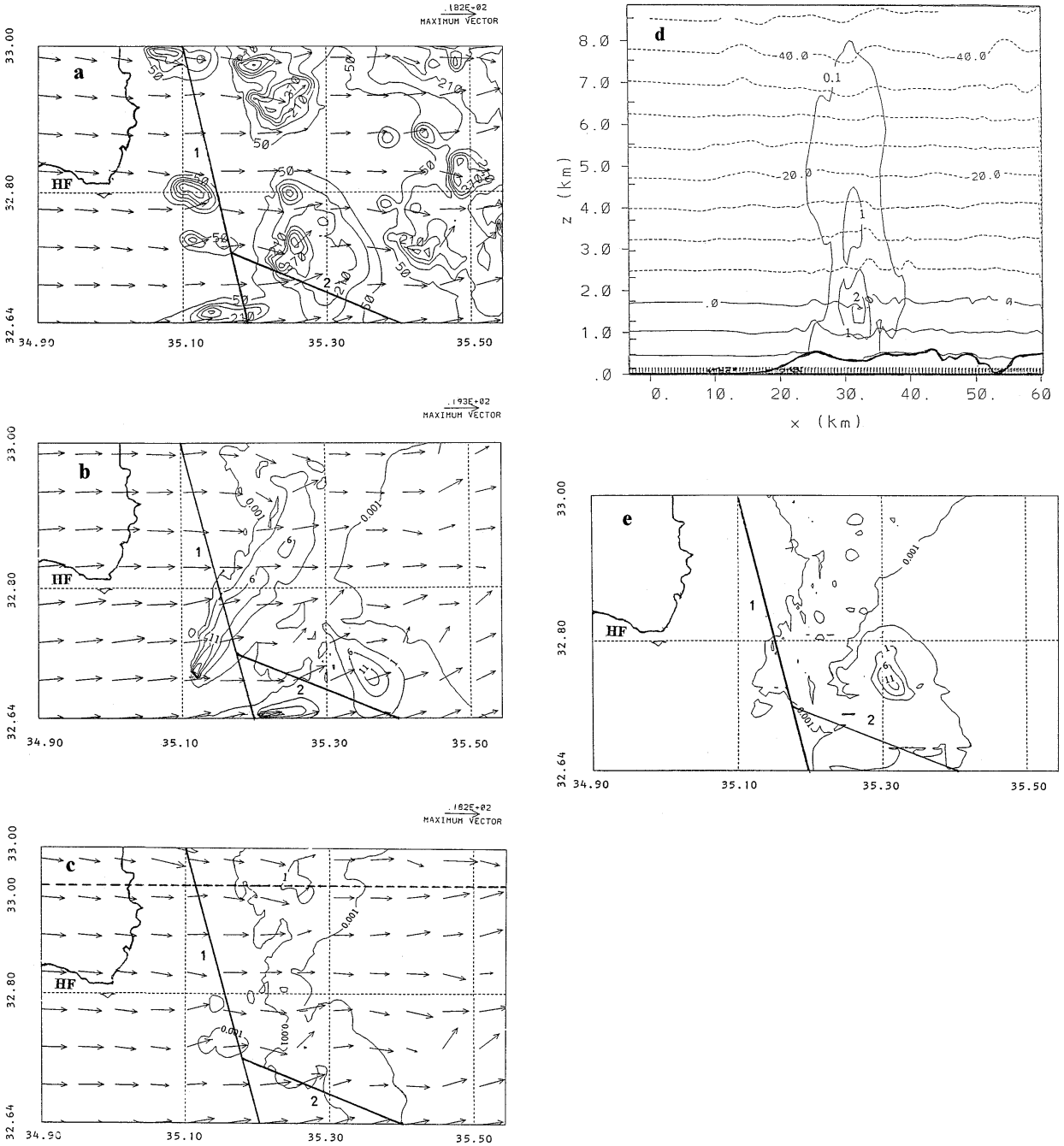

FIG. 3. (a) A horizontal cross section of total cloud condensate (water + ice + graupel) at 2961 m, showing the results of the simulation of case 1, 1 h from the beginning of the run. The contours have an interval of 0.8 g kg^{-1} starting from 0.5 g kg^{-1} (corresponding to the contours marked as 50). Maximum wind vector in all of Fig. 3 is 18.2 m s^{-1}. (b) Distribution of the concentration of seeding material at about 1300-m height after 1 h of simulation. The minimum contour marked 0.001 corresponds to 1 L^{-1}, and the contour marked 1 corresponds to a total concentration of 10^3 L^{-1} (1 L^{-1} active at -10°C). (c) Same as (b) but for 2961-m height after 1 h of simulation. The minimum contour is 1 L^{-1}. Heavy dashed line from west to east indicates the position of the cross section used for constructing (d). (d) A vertical cross section of the concentration of seeding material taken along the dashed line shown in (c), which runs through the region where the highest concentration of seeded particles reaches the upper levels of the cloud. Also shown are the isotherms, with solid and dashed curves representing temperatures higher and lower than 0°C, respectively. (e) Same as (a) but at an altitude of 466 m.

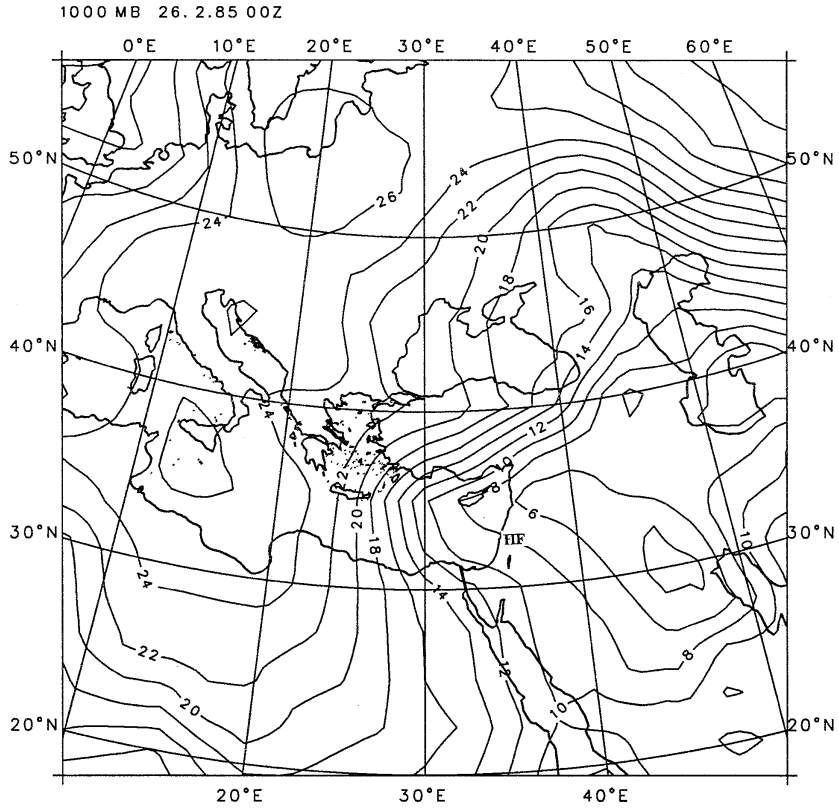

FIG. 4. Synoptic map of case 2 at 0000 UTC 26 February 1985 at 1000-hPa isobaric height. Isolines are presented every 2 hPa.

In this simulation, convective clouds penetrated the northern and central parts of Israel only about 3 h after the initiation of computations. Based on the criterion for seeding under these winds, particle release was simulated along two lines—the first over the northern part of the country (line 1) and the second over southern Israel (line 3).

1) SEEDING IN THE NORTH

Clouds were well developed over the central part of Israel, while another cloud group from the west was approaching the northern parts of the country. Seeding continued for 4 h, starting 3 h after the beginning of the integration. Figure 5a shows a horizontal cross section of the clouds in the finest grid in the northern area. The cross section is at a height of 2.9 km (~ -11°C) 1 h 45 min after seeding started. Cloud base was at about 1 km, with maximum condensate loading of about 2.1 g kg^{-1} located in the layer around 3500–4000 m over the target area (Fig. 5b). Figure 5c shows that at this time the only place where particles in concentrations of 10^3 to 6×10^3 L^{-1} were lifted to 2961 m was in the northernmost area of the simulation. A vertical cross section (Fig. 5d) of the tracer particles through the region of maximum concentration (line shown in Figs. 5a,c) about 1 h 45 min after seeding was initiated shows that 10^3 L^{-1} reached the upper levels (~ -15°C) in the clouds, where they could become effective as ice nuclei. However, in the temperature region where they could be most effective, namely, around $-8°$ to -12°C, only 1 L^{-1} was found.

2) SEEDING IN THE SOUTH

In the southern region, clouds penetrated from the sea, and seeding within the finest grid in the southern region was commenced about 3.5 h after the beginning of the simulation. Seeding along line 3 at 0400 UTC shows that the westerly winds with a small southerly component pushed the plume northward and somewhat parallel to the coast (Fig. 6a). At this stage, about 30 min after the beginning of seeding, the plane was still on its way south. About half an hour later the plane began its way back northward, and the plume, due to an intensification of the winds and a shift to a more westerly direction, was advected eastward, forming a line oriented in the east–west direction (Fig. 6b). Within the first 15–30 min from the initiation of seeding, only one cloud (not shown) in the northern edge lifted enough particles (10^3 L^{-1}, or 1 L^{-1} active at -10°C) to the -8°C level. About 1 h after the start of seeding, the clouds moved eastward (Fig. 6c). Comparing Fig. 6b with Fig. 6c, we see that the western part of the clouds was located

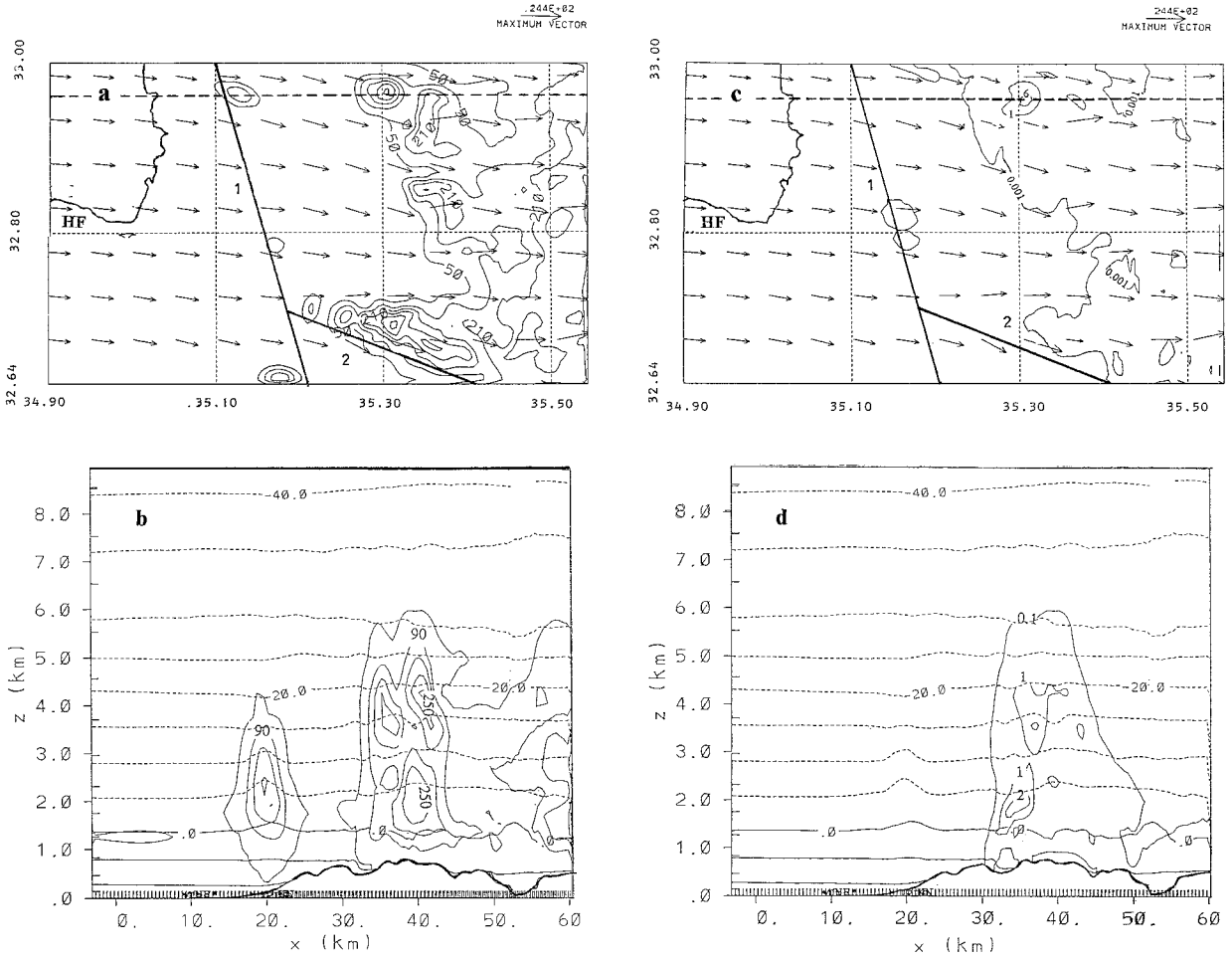

FIG. 5. (a) A horizontal cross section of the total condensate at about 2961 m, showing the results of the simulation of case 2 in the north, about 4 h 45 min from the beginning of the run. The contours are of cloud condensate with an interval of 0.8 g kg^{-1}, starting from 0.5 g kg^{-1}. The arrow on top is the scale for the maximum horizontal wind. The heavy dashed line represents the position of the cross section used for constructing (b) and (d). (b) A vertical cross section of the total condensate taken along the heavy dashed line shown in (a) and (c). The minimum contour is 0.5 g kg^{-1} with an interval of 0.8 g kg^{-1}. Also shown are the temperature isotherms. (c) A horizontal cross section of the particle concentration at 2961 m after 4 h and 45 min of seeding. As can be seen, only in one area did particles reach these levels in reasonable concentrations. The lowest contour is 1 L^{-1}. The heavy dashed line represents the position of the cross section used for constructing (b) and (d). (d) A vertical cut through the region in which the particle concentration was at a maximum [along the heavy dashed line in (a) and (c)]. The minimum contour value is 100 L^{-1}. Note that 10^3–2×10^3 L^{-1} reached $-10°$ to $-20°$C levels. Of these, only 1 L^{-1} is active at $-10°$C and about 10^2–10^3 L^{-1} are active at $-15°$ to $-20°$C, respectively.

downwind, but not far from, the place where the plane was present. At this point, the plume penetrated the cloud, and concentrations as high as 10^4 L^{-1} (or 10 L^{-1} active at $-10°$C) reached high altitudes (Fig. 6d).

5. Discussion

It should first be pointed out that the results presented here are at a resolution of 500 m. Somewhat similar results were obtained with only two nested grids, with the highest resolution being 3 km. The main difference in results between these two simulations was the lower concentrations of dispersed particles in the lower-resolution model. Such a difference could have been anticipated due to the averaging (smoothing) process that occurs at these resolutions. Unfortunately, no field experiment has yet been conducted to determine the concentrations of particles that actually reach the clouds. The simulations done here, therefore, have no measurement to be compared with, and the results should be viewed as suggestive guidelines for future experiments.

As pointed out before, the laboratory experiments carried out at CSU's cloud chamber using the AgI burners used in the field show that although ice nucleation begins at about $-6°$C (about 10^9 g^{-1}), the nucleation efficiency becomes significant only at temperatures lower than $-10°$C (10^{12} g^{-1}). It is clear, therefore, that not all the particles that reach this temperature level would immediately become effective; some may nucleate at much

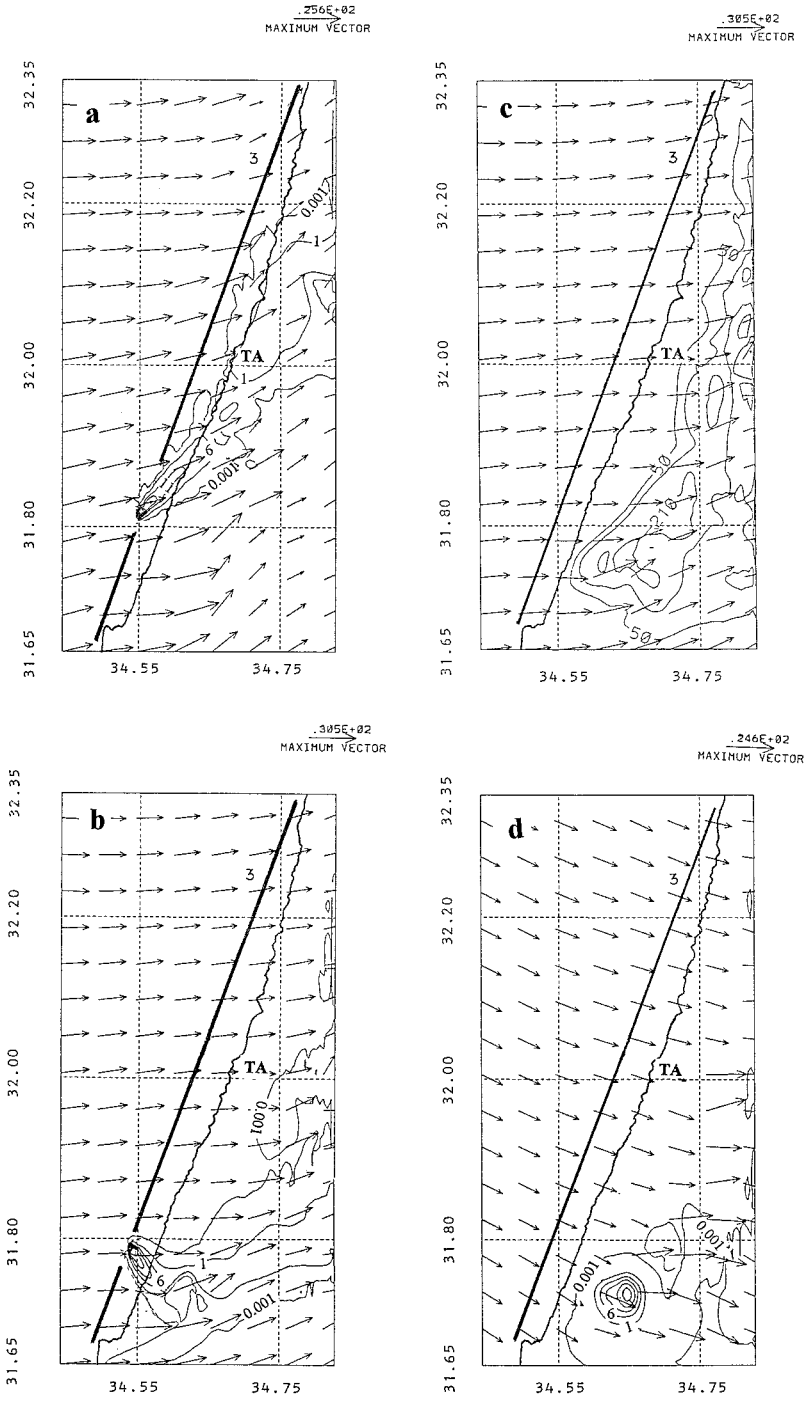

FIG. 6. (a) A horizontal cross section of the trace particles at 1300 m, 3.5 h after initiation of seeding in the southern region (case 2). Lowest contour is 1 L^{-1}. Solid line represents the position of seeding line 3. (b) Same as (a) but 30 min later. (c) The horizontal cross section of the total condensate at the same time as in (b). Although the clouds have moved eastward and away from the location of the seeding plane, some particles, though very few, were lifted into the clouds downwind of the seeding source. Minimum contour is 0.5 g kg^{-1}. (d) A horizontal cross section of the seeded particles at 2961-m altitude and at the same time as in (c). Minimum contour is 1 L^{-1} (corresponding to 0.001 in the figure).

lower temperatures (higher altitudes) or may not nucleate at all due to contamination. In examining the results, we should note that the numbers shown in the figures represent the total particle concentrations. For activation around -10°C, only about 10^{-3} out of these particles would be effective.

The experiments described in the previous sections suggest that cloud seeding using the broadcast static mode, as done in the Israeli project, can be effective in some cases, but it suffers from a number of difficulties. The results here suggest that much of the material released from the seeding plane is dispersed horizontally by the winds [similar conclusions were reached by Bruintjes et al. (1994) for particle dispersal over complex terrain]. A large fraction of it is forced downward by the downdrafts that are generated by precipitation from the clouds [see Tzivion et al. (1989) for the same effect in warm cloud seeding]. Considering that the present simulations do not include rainout or washout processes, it is reasonable to conclude that their inclusion would lead to a loss of a larger fraction of the dispersed material. In other words, the number concentration presented here represents an upper bound on what could be expected in nature.

The results also suggest that the criterion for seeding, based on wind direction at the 700-hPa level as it is measured at Beit Dagan in the central part of Israel, is generally correct. Even though some penetration of the seeded plume in the buffer region is seen in case 2, most of the particles remained below cloud base. The results also confirm the ongoing practice of preventing contamination of the buffer or the control areas by avoiding seeding on days for which the winds at the seeding levels and at 700 hPa are from the south-southwest.

In general, the simulations show that dispersing the seeding particles while the clouds are upwind (or downwind) of the seeding line does not assure that the particles get into the clouds. In many cases, the released particles moved with the winds at the seeding level and the location of the maximum concentration remained well ahead of (or behind) the main updrafts. Only some of the particles that got caught by the updrafts were lifted to higher levels. This was found to occur mostly when the updrafts passed above the seeding plane. There were a few cases (see Fig. 6d) in which the dispersed particles were advected eastward and ingested into the updrafts somewhere downwind of the source. A closer look, however, shows that the seeding plane was not far away from the core of the updraft, even though not exactly beneath it.

From the results of the present simulations, it seems that the only time when the particles reached the levels where they could be effective was when the clouds' updrafts passed over the seeding line while the plane was underneath or close by. The particles were found at the higher levels mostly in very localized regions, associated with the location of the updrafts. In these cases, the particles were lifted by the updrafts, undergoing mixing during their ascent. With the seeding rate of 500 g h^{-1}, the concentrations of the particles decreased to 10^3 to 5×10^3 L^{-1} at the $-8°$ to -10°C levels. In some cases, concentrations of over 10^3 L^{-1} were found all the way up to the upper parts of the clouds (with temperatures as low as -25°C). As pointed out before, however, most of these particles can form ice at temperatures as low as $-15°$ to -20°C. Only 10^{-3} of these particles could form ice at the levels where they are needed most (say around -10°C). It could be argued that introducing low concentrations of seeding agent at the -10°C level could only slightly enhance ice content at this level, but would leave enough particles to form ice at the higher altitudes and at lower temperatures, where they are not needed. In such cases, overseeding could occur—a process that could be detrimental to rain formation.

It is therefore clear that in the broadcast static seeding method, if sufficient concentrations of particles active at -10°C, say about 10–100 L^{-1}, are to be lifted to the $-8°$ to -10°C level, either a more efficient seeding agent must be used (more efficient by two orders of magnitude) or much larger amounts would have to be released (about 5–10 kg of AgI per hour). The use of such high concentrations of AgI would be much more expensive, would possibly require more elaborate dispersing techniques, and could also raise some environmental concerns.

It is possible, on the other hand, to change the seeding method and disperse the seeding material directly into the developing updrafts. Even though this would be a much costlier operation, requiring a much more elaborate system using radars and planes or rockets, it would be a much more effective method for ensuring that particles in the right concentrations get into the proper regions of the clouds.

Acknowledgments. We would like to thank Dr. J. K. Hall for providing us with the digitized topographical data, the Mekorot Water Company of Israel for their partial support of this work, and Professor P. Alpert for providing us with the ECMWF objective analysis data. Thanks are also due to Mr. and Mrs. L. Ross for their continued support of the work in the laboratory.

REFERENCES

Bruintjes, R. T., T. L. Clark, and W. D. Hall, 1994: Interactions between topographic airflow and cloud/precipitation development during the passage of a winter storm in Arizona. *J. Atmos. Sci.,* **51,** 48–67.

Dutton, J. A., and G. H. Fichtl, 1969: Approximate equations of motion for gases and liquids. *J. Atmos. Sci.,* **26,** 241–254.

Gabriel, K. R., and D. Rosenfeld, 1990: The second Israeli rainfall stimulation experiment: Analysis of rainfall on both target areas. *J. Appl. Meteor.,* **29,** 1055–1067.

Gagin, A., and J. Neumann, 1974: Rain stimulation and cloud physics in Israel. *Weather and Climate Modification,* W. N. Hess, Ed., Wiley-Intersciences, 454–494.

——, and ——, 1981: The Second Israeli Randomized Cloud Seeding

Experiment: Evaluation of the results. *J. Appl. Meteor.*, **20,** 1301–1311.

——, and M. Aroyo, 1985: Quantitative diffusion estimates of cloud seeding nuclei released from airborne generators. *J. Wea. Mod.*, **17,** 59–70.

Hall, J. K., 1993: DEMPACK: Dem data storage in a two-byte integer. *Comput. Geosci.*, **19,** 1567–1569.

Hallett, J., and S. C. Mossop, 1974: Production of secondary ice crystals during the riming process. *Nature*, **249,** 26–28.

Hussain, K., and C. P. R. Saunders, 1984: Ice nucleus measurements with a continuous flow chamber. *Quart. J. Roy. Meteor. Soc.*, **110,** 75–84.

Levin, Z., 1994: Aerosol composition and its effect on cloud growth and cloud seeding. *Sixth WMO Scientific Conf. on Weather Modification,* Paestum, Italy, World Meteor. Org. 367–370.

——, C. Price, and E. Ganor, 1990: The contribution of sulfate and desert aerosols to the acidification of clouds and rain in Israel. *Atmos. Environ.*, **24A,** 1143–1151.

Pielke, R. A., and Coauthors, 1992: A comprehensive meteorological modeling system—RAMS. *Meteor. Atmos. Phys.*, **49,** 69–91.

Rosenfeld, D., and H. Farbstein, 1992: Possible influence of desert dust on seedability of clouds in Israel. *J. Appl. Meteor.*, **31,** 722–731.

Tzivion, S., T. Reisin, Z. Levin, G. Feingold, and A. Manes, 1989: Dispersion of seeding material in clouds. *Proc. Fifth WMO Scientific Conf. on Weather Modification and Applied Cloud Physics,* Beijing, China, World Meteor. Org. 171–174.